Analysis of Low Reynolds Number Separation Bubbles Using Semiempirical Methods

Gordon S. Schmidt*
Loral Systems Group, Akron, Ohio
and
Thomas J. Mueller†
University of Notre Dame, Notre Dame, Indiana

The formation and growth of transitional separation bubbles can significantly affect boundary-layer development on airfoils operating at low chord Reynolds numbers. Of primary concern is the change in boundary-layer thickness between laminar separation and turbulent reattachment. This can be estimated using semiempirical methods, such as the one devised by H. P. Horton, which are based on solutions to the integral forms of the boundary-layer equations. The applicability of these methods at low Reynolds numbers was investigated using hot-wire measurements of bubbles formed on an NACA 66_3-018 airfoil at chord Reynolds numbers of 50,000–200,000. Analysis of the data revealed significant Reynolds number effects on the evolution of separated laminar flow. The momentum thickness growth between separation and transition was found to be similar to that predicted for a laminar half-jet and appears to be influenced by the momentum thickness Reynolds number at separation. This parameter also was found to have a noticeable effect on the Reynolds number based on the length of a bubble's laminar portion. In the turbulent portion of the bubbles, no Reynolds number effects were evident. This was true for both the momentum thickness growth and for Horton's reattachment criterion.

Nomenclature

B = $(R_{\delta_2})_S \tan\gamma$
C = airfoil chord length
C_d = dissipation coefficient, $(2/\rho U^3)\int_0^\delta \tau(\partial u/\partial y)\,dy$
C_f = local skin-friction coefficient, $(2\nu/U^2)(\partial u/\partial y)_{y=0}$
E_1 = function used to define C_d in laminar flow, $2\int_0^{\delta/\delta_2}[\partial(u/U)/\partial(y/\delta_2)]^2\,dy/\delta_2$
H_{12} = δ_1/δ_2
H_{32} = δ_3/δ_2
H_∞ = δ_∞/δ_2
k = constant used in formulation for $(\delta_3)_T$
L_S = macroscale of freestream turbulence
l_1 = length of separation bubble's laminar region, $x_T - x_S$
R_C = chord Reynolds number, $\rho U_\infty C/\mu$
R_{l_1} = $\rho U_S l_1/\mu$
R_{δ_2} = $\rho U_S \delta_2/\mu$
T = root-mean-square of turbulent fluctuations in freestream
U = velocity component parallel to airfoil's surface at edge of boundary layer
U_∞ = freestream velocity
u = velocity component parallel to airfoil's surface at a point within the boundary layer
v = velocity component normal to airfoil's surface at a point within the boundary layer
x = distance along airfoil's surface, usually measured from leading edge
y = distance from airfoil's surface along a line normal to surface
y_D = y location of dividing streamline
α = airfoil angle of attack
γ = angle between dividing streamline and airfoil surface near separation point
Δ = difference between two quantities
δ = boundary-layer thickness
δ_1 = boundary-layer displacement thickness, $\int_0^\delta (1 - u/U)\,dy$
δ_2 = boundary-layer momentum thickness, $\int_0^\delta (u/U)(1 - u/U)\,dy$
δ_3 = boundary-layer energy thickness, $\int_0^\delta (u/U)[1 - (u/U)^2]\,dy$
δ_∞ = boundary-layer entrainment thickness, $\delta - \delta_1$
θ = thickness of separated shear layer, $y_{u/U=0.9} - y_{u/U=0.1}$
Λ_R = $(\delta_2/U)_R\,(dU/dx)_R$
μ = absolute viscosity of air
μ_t = eddy or virtual viscosity, $-\rho\overline{u'v'}/(\partial u/\partial y)$
ν = kinematic viscosity of air, μ/ρ
ξ = $(x - x_S)/[(\delta_2)_S(R_{\delta_2})_S]$
ρ = air density
τ = turbulent shear stress, $-\rho\overline{u'v'} + \mu(\partial u/\partial y)$

Subscripts

m = mean value over bubble's turbulent portion
R = value of subscripted variable at reattachment
S = value of subscripted variable at laminar separation
T = value of subscripted variable at transition

Introduction

ALTHOUGH the majority of airfoil applications are associated with chord Reynolds numbers on the order of 10^6 to 10^7, a number of applications exist that require efficient operation for R_C less than 1×10^6. Two examples of low Reynolds number applications[1] are automotive gas turbine blades and the wings of remotely piloted vehicles for which R_C ranges are 29,000–187,000.[1] These low values are the result of small physical dimensions and low operating speeds. There are also cases in which low fluid density contributes to small values of R_C. For example, small axial-flow fans used to cool electronic equipment in the unpressurized compartments of high-altitude aircraft[2] might operate at a chord Reynolds number of only 3000.[2]

Several problems have arisen in the development of efficient airfoils for these applications. For example, conventional airfoil design strategies seek to control the onset and develop-

Received March 7, 1988; revision received Sept. 6, 1988.

*Graduate Research Assistant; currently Senior Development Engineer. Member AIAA.
†Professor, Department of Aerospace and Mechanical Engineering. Associate Fellow AIAA.

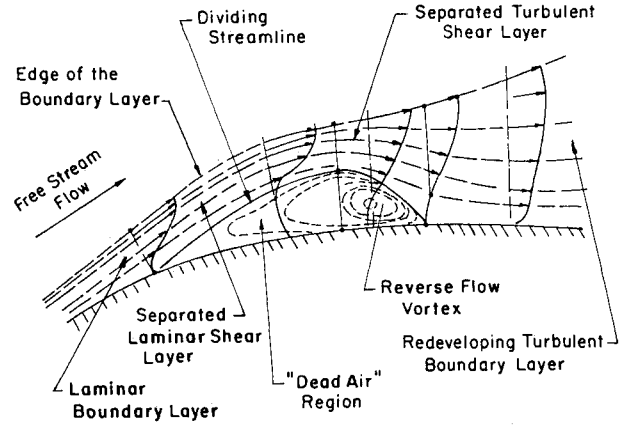

Fig. 1 Flowfield in the vicinity of a transitional separation bubble.[3]

ment of turbulent boundary layers. This becomes difficult at low Reynolds numbers due to the increased stability of the attached laminar boundary layers. As a result, laminar separation is common on airfoils operating at low Reynolds numbers, even at small angles of attack. The development of a turbulent boundary layer under these conditions may depend on the formation of a transitional separation bubble (Fig. 1). This flow phenomenon involves the separation of a laminar boundary layer, followed by transition of the highly unstable separated shear layer. Turbulent mixing then results in reattachment of the shear layer. However, the turbulent boundary layer that develops downstream of the separation bubble is usually thicker than one formed in an attached transition process. This will result in increased drag and may lead to premature separation of the turbulent boundary layer. In order to predict these effects, the boundary-layer characteristics at reattachment must be accurately determined. On the other hand, the complexity of airfoil flows at low Reynolds numbers may be great enough that fairly simple methods must be used to model the variety of phenomena that can occur simultaneously. For example, a typical flowfield about a low Reynolds number airfoil could include a transitional separation bubble on the airfoil's upper surface close to the leading edge and regions of separated flow near the trailing edge. Because separated trailing-edge flow has a substantial effect on an airfoil's overall surface pressure distribution, an elaborate iterative viscous-inviscid technique probably would be needed to accurately calculate this effect. However, the separation bubble's influence on the pressure distribution may be only locally significant. If this is the case, then its primary effect is on the turbulent boundary layer. In order to account for this effect, at least two pieces of information must be determined. First, the location of turbulent reattachment is needed as the starting point for computing the development of the turbulent boundary layer along the airfoil's surface. Second, the boundary-layer characteristics at reattachment are needed. These would serve as initial conditions in a turbulent boundary-layer computation scheme.

During the past two decades, simple semiempirical methods have evolved that may be able to predict the above-mentioned characteristics of two-dimensional transitional separation bubbles with sufficient accuracy. The methods consist of relationships between various bubble characteristics and the boundary-layer properties at the point of laminar separation. These relationships are based on analyses of the integral forms of the boundary-layer equations and depend upon several assumptions concerning the form of the surface pressure distribution and the nature of the flow in the vicinity of a separation bubble. However, these relationships also depend on experimental data that has been obtained at high Reynolds numbers. The object of this article is to review the semiempirical separation bubble methods and to test their generality using measurements obtained primarily at chord Reynolds numbers between 50,000 and 200,000.

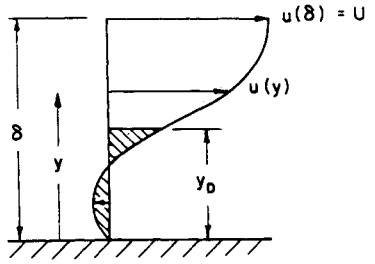

Fig. 2 Nomenclature for separated flow velocity profiles.

Characteristics of Separation Bubbles

The major features of flow in the vicinity of transitional separation bubbles are shown in Fig. 1. Downstream of the laminar separation point, a wedge of recirculating fluid develops that is bounded by the airfoil surface and the separated shear layer. This fluid wedge makes up the laminar portion of the separation bubble. The magnitude of reverse-flow velocities in this region is typically very small, on the order of a few percent of that at the edge of the shear layer. The displacement effect of this wedge of fluid on the external flow causes a reduction in the adverse pressure gradient that would exist if the bubble were absent. In many cases, the gradient in surface pressure (and external velocity) in this region is reduced approximately to zero. Once transition of the separated shear layer has occurred, momentum exchange across this layer by the turbulent mixing process reduces the vertical extent of the reverse-flow layer and also the displacement effect of the bubble. A deceleration of the external flow over the bubble's turbulent portion results with an accompanying adverse pressure gradient. The magnitude of the reverse-flow velocities are much larger in this region, on the order of 20% of U.[3] If the bubble is small relative to the airfoil's chord, the external velocities at the separation and reattachment points are nearly equal to those that would be present at those locations if no bubble had formed. This type of separation bubble is generally referred to as a "short bubble." If the local Reynolds number is low enough and the pressure gradient is sufficiently steep, the turbulent mixing process is unable to produce flow reattachment. Under these conditions, the bubble "bursts": separated flow extends over much of the airfoil, which causes the airfoil's pressure distribution to collapse. Since this also causes a reduction in the adverse pressure gradient, reattachment eventually may take place. The length of the resulting "long" bubble can be on the order of the airfoil's chord.

Separation Bubble Measurements at Low Reynolds Numbers

Most of the data that will be discussed was derived from hot-wire anemometry measurements of "short" separation bubbles formed at the leading edge of an NACA 66_3-018 airfoil. These measurements were obtained by O'Meara using the equipment and procedures described in Ref. 4. Data were acquired at chord Reynolds numbers of 50, 80, 100, 140, 160, and 200×10^3 and at angles of attack of 10 and 12 deg. In addition, the freestream turbulence intensity was varied at a constant value of R_C through the use of flow restrictors. A flow restrictor consists of a frame packed with plastic drinking straws that is covered on both ends by wire mesh. The effect of mounting one or two flow restrictors between the test section and diffuser of the nonreturn wind tunnel was to increase the turbulence at a given airspeed.

One of the difficulties in analyzing the data was that it was obtained using a single-wire sensor. This meant that only the magnitude of the local flow velocity could be measured. Now, the locations of laminar separation and turbulent reattachment are interfaces between regions of forward and reverse flow. Therefore, the hot-wire probe's inability to indicate flow direction complicated the determination of these locations. Also, it is difficult to accurately calculate the integral parame-

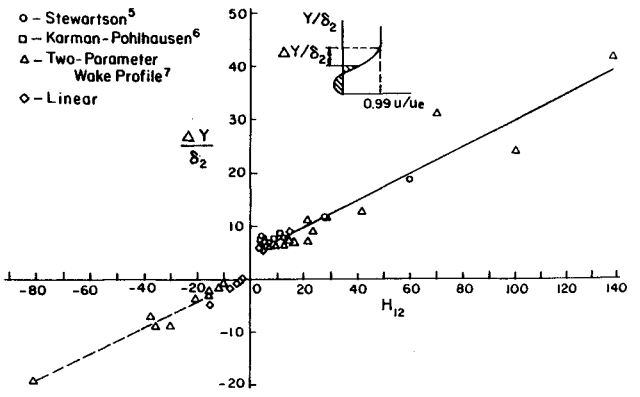

Fig. 3 Separated shear layer thickness correlation.

ters (δ_1, δ_2, δ_3, H_{12}, and H_{32}) without precise knowledge of the flow direction inside a bubble. For example, consider the velocity profile in Fig. 2. The momentum thickness is defined as

$$\delta_2 = \int_0^{\delta} (u/U)(1 - u/U)\, dy \tag{1a}$$

$$\delta_2 = \int_0^{y_D} u/U\, dy + \int_{y_D}^{\delta} u/U\, dy - \int_0^{\delta} (u/U)^2\, dy \tag{1b}$$

The first integral is zero since it defines the net mass flow in the recirculation region. However, if u/U is treated as positive across the layer, this integral will not equal zero, and δ_2 will be determined to be larger than it actually is. The energy thickness δ_3 will also experience a fictitious growth, whereas the displacement thickness δ_1 will be reduced. The increments in δ_1, δ_2, and δ_3 are

$$\Delta\delta_1 = -\int_0^{y_D} |u/U|\, dy \tag{2}$$

$$\Delta\delta_2 = \int_0^{y_D} |u/U|\, dy \tag{3}$$

$$\Delta\delta_3 = \int_0^{y_D} |u/U|\, [1 - (u/U)^2]\, dy \tag{4}$$

For the case of a simple linear velocity profile, it was found[1] that the increase in δ_2 and δ_3 could exceed 100% at values of H_{12} greater than 10. However, the displacement thickness was reduced by no more than 20%.

In order to eliminate these uncertainties, a technique was sought that could determine the height of the dividing streamline y_D from the experimental velocity profiles. From Eq. (1b), it can be seen that δ_2 decreases as y_D increases. Since the quantity $\delta - y_D$ also decreases, it was hypothesized that the ratio $(\delta - y_D)/\delta_2$ might remain constant. This hypothesis was tested by computing the ratio for a variety of analytical velocity profiles exhibiting reverse flow. The results are shown plotted against H_{12} in Fig. 3. In general, the ratio of the separated shear layer thickness to the momentum thickness varies a great deal with H_{12}. However, in the range of H_{12} applicable to separation bubbles (about 3-17), this ratio is approximately constant and equal to 7. The standard deviation for the 37 points within this range is 0.8. Linear least square fits for the entire data set are

$$\Delta y/\delta_2 = 4.9410 + 0.2534\, H_{12}, \quad 3.00 \le H_{12} \le 137.5 \tag{5a}$$

$$\Delta y/\delta_2 = 0.7384 + 0.2418\, H_{12}, \quad -81.25 \le H_{12} \le -3.00 \tag{5b}$$

where Δy is the distance from the dividing streamline to the point at which $u/U = 0.99$. These relationships then were used to determine y_D for the experimental velocity profiles in the vicinity of O'Meara's separation bubbles. It was assumed

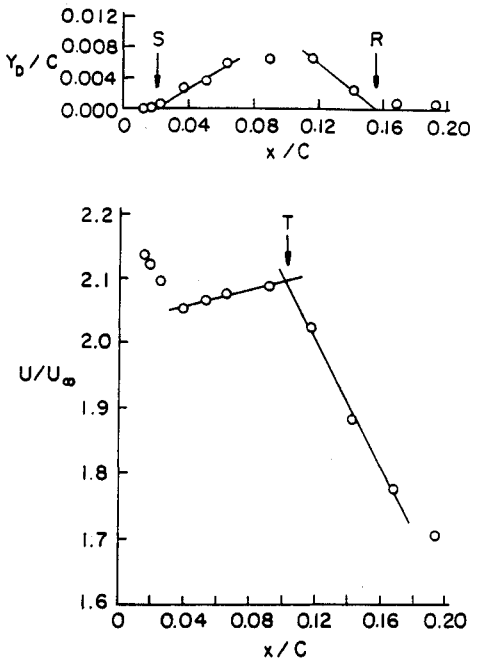

Fig. 4 Dividing streamline shape and external velocity distribution (R_c = 80,000, α = 12 deg, one flow restrictor).

the y_D coincided with the data point in each profile for which H_{12} and $\Delta y/\delta_2$ best satisfied Eq. (5a) or (5b). An example of the resulting dividing streamline shapes is shown in Fig. 4. This shape is very similar to those obtained by more sophisticated means of flow measurement. The positions of separation and reattachment were determined from the y_D vs x data as shown in the figure. Also shown in Fig. 4 is the corresponding external velocity distribution. The location of transition was assumed to lie at the end of the velocity plateau, with Ref. 8.

Analysis of Separation Bubble Measurements

Overview of Semiempirical Methods

A necessary assumption of the semiempirical methods is that Prandtl's boundary-layer equations are valid in small regions of separated flow. This, in turn, requires $\partial p/\partial y$ and v to be negligible, which—at least in the latter case—is not true at all points within the separation bubble. Nevertheless, solutions of the equations have been obtained for this type of separated flow that agree very well with experiments.

The semiempirical methods usually seek solutions to the following integral forms of the boundary layer equations:

Conservation of momentum:

$$\frac{d\delta_2}{dx} + (H_{12} + 2)\frac{\delta_2}{U}\frac{dU}{dx} = \frac{C_f}{2} \tag{6a}$$

Conservation of mechanical energy:

$$\frac{d(U^3\, \delta_3)}{dx} = C_d\, U^3 \tag{6b}$$

These equations are solved by using an assumed form for the external velocity distribution $U(x)$ and assumed values for the parameters H_{12}, C_f, and C_d. Initial conditions are obtained by calculating the boundary-layer characteristics at the point of laminar separation. This is accomplished by using conventional integral methods. It should be noted that the accurate prediction of laminar separation is not always an easy task since it requires an accurate definition of $U(x)$ upstream of separation.

Laminar Portion of Transitional Separation Bubbles

Horton[3] characterized the flow within a bubble's laminar region as essentially stagnant. Thus, he argued that the skin

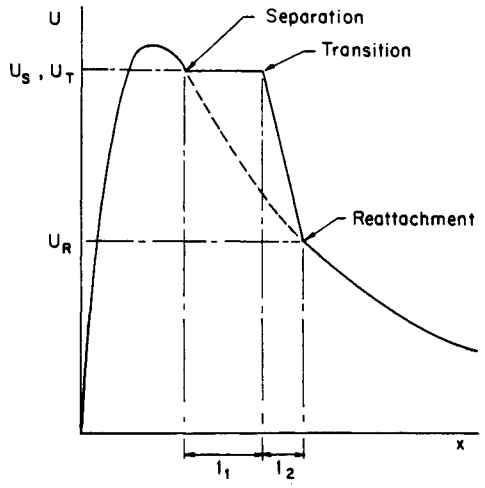

Fig. 5 Horton's model of the external velocity distribution in the vicinity of a separation bubble.[3]

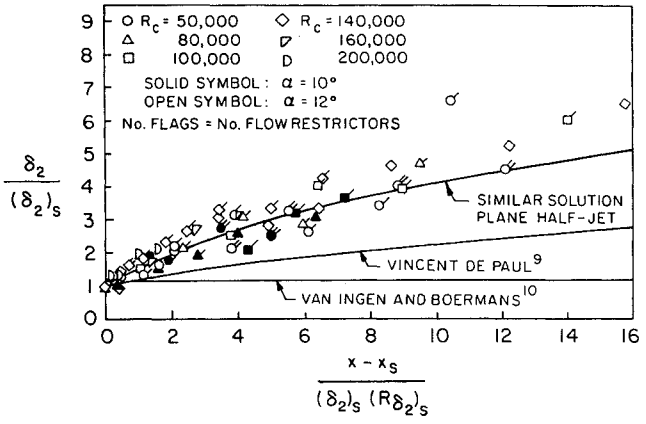

Fig. 6 Momentum thickness growth in the laminar portion of transitional separation bubbles.

friction was negligible. In addition, according to his assumed external velocity distribution (Fig. 5), $dU/dx = 0$. From Eq. (6a), it was concluded that $d\delta_2/dx$ is equal to zero. Therefore, the momentum thickness at transition must be the same as at separation. On the other hand, Vincent de Paul[9] argued that Eq. (6b) be used instead of Eq. (6a) to calculate $\delta_2(x)$ in regions of separated flow since it was less sensitive to variations in static pressure across the viscous layer. Using the laminar self-similar velocity profiles of Stewartson,[5] he defined C_d as a function of y_D, δ_1, and R_{δ_2}

$$C_d = \frac{E_1(y_D/\delta_1)}{R_{\delta_2}} \tag{7}$$

Multiplying Eq. (6b) by $U^3\delta_3$, he obtained

$$\frac{1}{2}\frac{d(U^6\delta_3)}{dx} = \nu\,(H_{32}E_1)\,U^5 \tag{8}$$

Since $H_{32}E_1$ was approximately constant for $y_D/\delta_1 < 0.8$, this parameter was assumed equal to its value at separation ($y_D/\delta_1 = 0$). Equation (8) then was evaluated for two different $U(x)$ distributions, which yielded

$$\frac{(\delta_3)_{T2}}{(\delta_3)_{S2}} \approx 1 + 6\frac{\Delta U}{U_S} + 2\left(\frac{E_1}{H_{32}}\right)_S\left(1 + k\frac{\Delta U}{U_S}\right)\frac{l_1}{(\delta_2)_S(R_{\delta_2})_S} \tag{9}$$

where k is equal to 1 when $U/U_S = 1 - \Delta U/U_S$ and is equal to 6 when U/U_S varies linearly between 1 and $(1 - \Delta U/U_S)$ as x ranges from x_S to x_T. The constant 2 $(E_1/H_{32})_S$ is equal to 0.41. Since H_{32} is nearly constant in regions of separated flow, Vincent de Paul's expression for the ratio $(\delta_3)_{T2}/(\delta_3)_{S2}$ also applies to the ratio $(\delta_2)_{T2}/(\delta_2)_{S2}$.

A somewhat different method was employed by van Ingen and Boermans[10] to predict $\delta_2(x)$ in the laminar portion of separation bubbles. They suggested, on the basis of a limited number of experiments, that the external velocity in the laminar region could be described by the following formula:

$$U/U_S = 0.978 + 0.022\exp(-4.545\xi - 2.5\xi^2)$$

$$0 \le \xi \le 1.3333 \tag{10a}$$

$$U/U_S = 0.978, \qquad \xi \ge 1.3333 \tag{10b}$$

Using Eq. (6a) in addition to relationships between characteristic parameters bases on the Stewartson velocity profiles, an expression for the momentum thickness was derived:

$$\frac{\delta_2}{(\delta_2)_S} = \{1 + 0.152[1 - (1 - 0.75\xi)^4]\}^{1.25}, \quad 0 \le \xi \le 1.3333 \tag{11a}$$

$$\frac{\delta_2}{(\delta_2)_S} = 1.1935, \qquad \xi \ge 1.3333 \tag{11b}$$

Another approach to analyzing the momentum thickness growth downstream of separation is to draw an analogy between the separated shear layer and the free shear layer produced by the interaction of a wide, uniform jet with a region of stagnant fluid.[1,11] In both cases, a pressure gradient does not exist or is negligible. The major difference between the two types of flow is that the separated shear layer interacts with a solid boundary (the airfoil surface). The velocity profiles in the free shear layer are self-similar and can be determined by solving the boundary-layer equations in an analogous manner to the solution for flow along a flat plate. The momentum thickness of the resulting profile[12] is

$$\delta_2 = 1.241\sqrt{\nu x/U} \tag{12}$$

This equation can be rearranged to yield the momentum thickness at some position in terms of the momentum thickness at a reference location. For flow in a separation bubble's laminar region, the obvious choice for the reference location is the separation point. Hence, δ_2 can be computed in terms of $(\delta_2)_S$ using the formula

$$\delta_2/(\delta_2)_S = \sqrt{1 + (1.241)^2(x - x_S)/[(\delta_2)_S(R_{\delta_2})_S]} \tag{13}$$

This result reveals a dependency of $\delta_2/(\delta_2)_S$ on the parameter $(x - x_S)/[(\delta_2)_S(R_{\delta_2})_S]$, as did the formulas of Vincent de Paul and van Ingen. The momentum thickness growth predicted by Eq. (13) is considerably greater than that predicted by the other two equations, however.

In Fig. 6, the momentum thickness data derived from O'Meara's experiments has been plotted along with the curves defined by Eqs. (9), (11), and (13). The velocity difference between separation and transition, $\Delta U/U_S$, used in Eq. (9) was assumed to be zero. Actually, examination of the hot-wire data revealed that $\Delta U/U_S$ ranged from -0.0220 to 0.0439. In all likelihood, values of this magnitude should have little impact on the computation of $\delta_2/(\delta_2)_S$. The implications of Fig. 6 are fairly significant. First, the momentum thickness displays a rather large growth that is not predicted by Eqs. (9) and (11). Equation (13) is more successful in predicting the momentum thickness growth for values of $(x - x_S)/[(\delta_2)_S(R_{\delta_2})_S]$ less than 6 but tends to underestimate $\delta_2/(\delta_2)_S$ for larger values. This additional growth may be caused by turbulent stresses that develop as the flow begins to transition. Another important implication is that the growth in δ_2 over the laminar portion of bubbles at low Reynolds numbers is as great as the overall growth between separation and reattachment at much higher

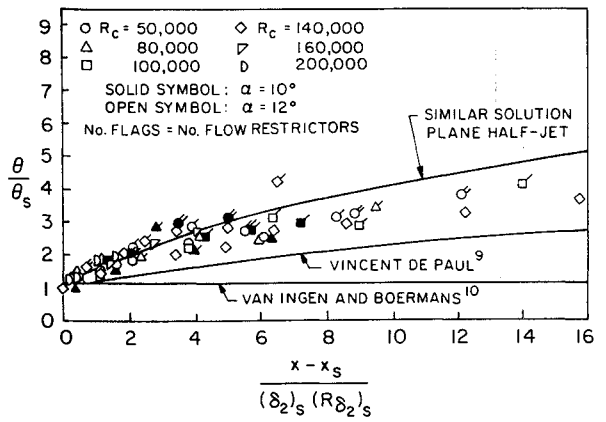

Fig. 7 Shear layer thickness growth in the laminar portion of transitional separation bubbles.

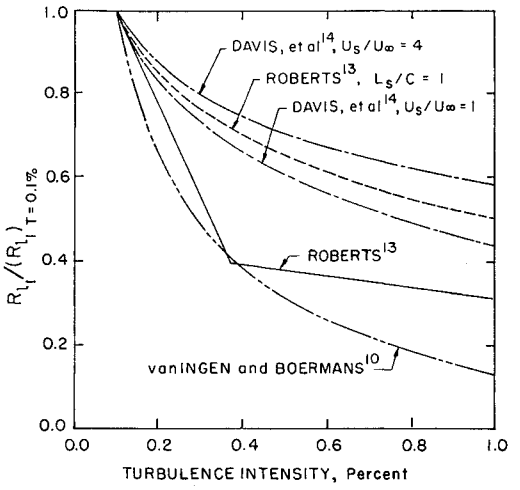

Fig. 8 Sensitivity of the transition Reynolds number to freestream turbulence intensity.

Reynolds numbers. This suggests that substantial drag penalties could result from separation bubbles at low Reynolds numbers.

The momentum thickness data used in the preparation of Fig. 6 were obtained from velocity profiles corrected to account for the presence of reverse flow. Since there was some doubt whether the momentum thicknesses had been calculated properly, the above observations were tested using a different approach. In Fig. 7, the separated shear layer thickness θ has been plotted as a function of the similarity parameter $(x-x_S)/[(\delta_2)_S(R_{\delta_2})_S]$. This test was based on Roberts' observation that the velocity profiles in a separated shear layer are similar in shape.[13] Therefore, θ/θ_S should be approximately equal to $\delta_2/(\delta_2)_S$. Here, θ is the shear layer thickness measured from the point where u/U equals 0.1 to the point where u/U is equal to 0.9. This definition was originally used by Roberts in his investigation of velocity profile similarity. Figure 7 provides additional evidence that the momentum thickness does indeed experience a large growth in the laminar region of separation bubbles. Note that Eq. (13) represents the growth in θ reasonably well for values of $(x-x_S)/[(\delta_2)_S(R_{\delta_2})_S]$ less than 6 as in the case of δ_2. For larger values, however, this formula consistently overpredicts the growth in θ. It is apparent that θ/θ_S is not exactly equal to $\delta_2/(\delta_2)_S$, which indicates that the velocity profiles in the separated shear layer are not exactly self-similar. The increasing disparity between θ/θ_S and $\delta_2/(\delta_2)_S$ as $(x-x_S)/[(\delta_2)_S(R_{\delta_2})_S]$ increases is probably due to a growing deviation of the profiles from the shape at separation.

Laminar-to-Turbulent Transition

One of the distinguishing features of "short" separation bubbles is that laminar flow exists over a large fraction of their

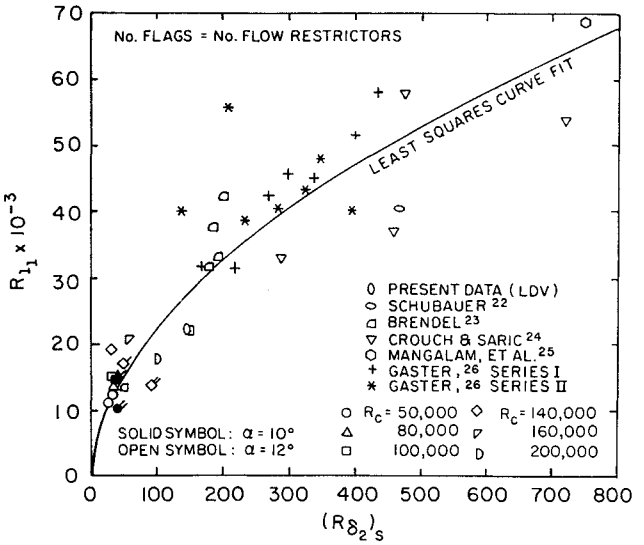

Fig. 9 Effect of the momentum thickness Reynolds number at separation on the transition Reynolds number.

total length. Typically, l_1/l ranges from 0.6 (Ref. 3) to as much as 0.85 (Ref. 8). This fact and the findings reported in the previous section suggest that l_1 must be accurately determined in order to successfully predict the location of flow reattachment and the boundary-layer growth between separation and reattachment.

In Horton's analysis of separation bubbles, l_1 was characterized by a transition Reynolds number R_{l_1}. Using data obtained by fellow researchers at Queen Mary College, he found that R_{l_1} ranged between 30,000 and 50,000. An uncertainty of 12% was assigned to the measurements, leaving a substantial variation in the data about the mean value of 40,000. This was attributed to differences in the level of fluctuations present in the separating boundary layers. In order to account for this factor, several empirical correlations between R_{l_1} and measures of freestream turbulence have been developed.[10,13,14] These correlations are shown plotted in Fig. 8. The significant differences between the correlations indicates that other factors may be influencing R_{l_1}.

It has been suggested that the role of freestream turbulence in the transition process is to control the rate at which a broad spectrum of disturbances feed on those that have been amplified as a result of flow instability.[15] Several factors have been shown to affect the initial growth of small disturbances within a separated shear layer. These are 1) the distance between shear layer and solid boundary, 2) shape of shear layer velocity profile, 3) local shear layer thickness, and 4) local Reynolds number. These factors have been included by Crimi and Reeves[16] in a transition criterion based on an analogy to roughness-induced transition. They hypothesized that transition would occur when a critical value of the local Reynolds number was exceeded, which in turn depended on the height of the separated shear layer above the airfoil surface. Venkatesworlu and Marsden[17] have devised a similar criterion that involved the height of the separation bubble at transition. In Ref. 1, these criteria were recast into a form involving R_{l_1},

$$R_{l_1} \propto (B \times H_{12})_S^{-1} \tag{14}$$

Both the separation angle parameter B and $(H_{12})_S$ have been found to depend on the pressure distribution upstream of separation.[1,18] Typically, B ranges[19] from 15-20, and $(H_{12})_S$ usually lies[18] between 3.1 and 4.0. This variation is certainly great enough to explain the scatter in R_{l_1} noted by Horton. However, Dryden[20] has reported that R_{l_1} can range from 2000 to as much as 380,000. Such a broad range would be difficult to account for even by combining the effects of freestream turbulence with variations in B and $(H_{12})_S$.

Table 1 Range of parameters in transition correlation data base

Source	$(R_{\delta_2})_S$	$(H_{12})_S$	T, %	B	$R_{l_1} \times 10^{-4}$
O'Meara[4]	27.7–100.3	2.5–4.0	0.11–0.30	2.6–19.4	1.0–2.1
Schubauer[22]	468.0	3.4	0.85	—	4.0
Brendel[23]	52–203	3.1–3.5	0.044	5.1–13.7	1.3–4.2
Crouch and Saric[24]	287.7–720.2	2.9–4.3	0.05	—	3.3–5.8
Mangalam et al.[25]	748.3	—	0.025	20.38	6.9
Gaster,[26] series I	167–432	—	0.05	—	3.2–5.8
Gaster,[26] series II	136–394	—	0.05	—	3.9–5.6

In addition to B, $(H_{12})_S$, and freestream turbulence, the Reynolds number at separation $(R_{\delta_2})_S$ has been found to influence R_{l_1}. Woodward[21] suggested the following correlation:

$$R_{l_1} = A_0(R_{\delta_2})_S^2 + B_0 \tag{15}$$

where A_0 and B_0 are functions of the pressure distribution. However, no generally applicable forms were established for the functions. Vincent de Paul[9] also noticed the effect of $(R_{\delta_2})_S$ on R_{l_1}, finding that R_{l_1} tends to increase with increasing $(R_{\delta_2})_S$.

In Fig. 9, R_{l_1} has been plotted against $(R_{\delta_2})_S$ using data obtained from several sources. Although a good deal of scatter is evident, there does appear to be a definite relationship between the two parameters. A least squares curve fit of this data yielded the following formula:

$$R_{l_1} = 2175\ (R_{\delta_2})_S^{0.5150} \tag{16}$$

Of the 38 points used in the correlation, 17 lie with 10% of the curve represented by this equation. Twenty-six lie within 20% of the curve. At least three factors may be responsible for the scatter. First, the locations of separation and transition, which were needed to determine R_{l_1}, were established using a variety of techniques. The methods used to extract separation and transition locations from O'Meara's hot-wire measurements have been described already. Other techniques represented by the data in Fig. 9 involved the following types of measurements: surface flow visualization,[22] velocity contours,[23,26] integral boundary layer parameters,[23,25] turbulence measurements,[24–26] seed particle velocity component histograms,[25] and mean velocity profiles.[25,26] These techniques are unquestionably useful in determining the extent of laminar flow in a separation bubble. However, it is not clear whether the values of R_{l_1} based on these different methods represent the same stage in the laminar-to-turbulent evolution of a separated shear layer. An appreciation for the differences in R_{l_1} that can result from using different methods to determine transition can be gained by examining the data published in Ref. 26. Values of R_{l_1} determined by associating transition with the end of the pressure plateau differed from the reported values (which apparently were based on the shape of velocity contours) by no more than 12.6% in 12 of the 14 cases. Although this difference is not large, it does suggest that some of the scatter evident in Fig. 9 may be attributed to differences in the techniques used to determine R_{l_1}. Uncertainties due to the spacing between measurement stations also may be responsible for some of the data scatter. According to Ref. 23, the uncertainties in determining the locations of laminar separation and transition were ± 0.005 and $\pm 0.015C$, respectively. The resulting uncertainties in R_{l_1} were 7.1–24.8%. Reference 24 reported an uncertainty in R_{l_1} of ± 5000, which yielded uncertainties of 8.6–15.2%. Finally, the variations in B, $(H_{12})_S$, and freestream turbulence intensity associated with the data shown in Table 1 are probably also responsible for the scatter.

For a given pressure distribution about an airfoil, Reynolds numbers based on measures of the local boundary-layer thickness (such as δ_1 and δ_2) are proportional to $R_C^{1/2}$.[27] Therefore, Eq. (16) implies that R_{l_1} is proportional to $R_C^{0.2575}$ at a constant angle of attack. This shows that the transition Reynolds number is not highly sensitive to small variations in the chord Reynolds number. This result also shows the danger in using values of R_{l_1} based on high Reynolds number data to predict the location of transition on a low Reynolds number airfoil. For example, over a chord Reynolds number range of 10^5–10^6, R_{l_1} varies by a factor of 1.8. It should be pointed out, however, that variations in the airfoil's pressure distribution will occur at a constant angle of attack over such a broad Reynolds number range due to interactions between the boundary layer and the external flow. These variations may tend to reduce the differences in $(R_{\delta_2})_S$ and, as a result, R_{l_1}.

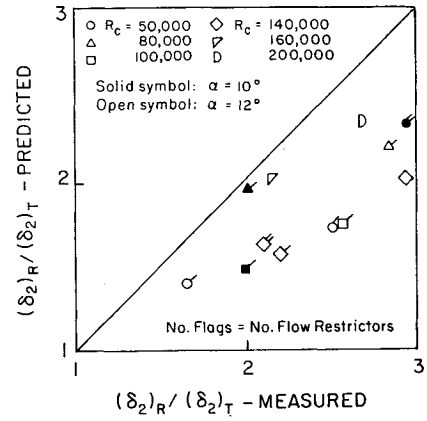

Fig. 10 Measured growth in momentum thickness over bubble's turbulent portion compared with predicted growth using Horton's recommended value for the dissipation coefficient, $(C_d/H_{32})_m = 0.0121$.

Turbulent Portion of Transitional Separation Bubbles

The growth in momentum thickness over a bubble's turbulent region has been treated in a similar manner by Horton and Vincent de Paul. Equation (6b) is integrated assuming constant values for C_d and H_{32} and a linear decrease in U between transition and reattachment. The resulting formula is

$$(\delta_2)_R = (\delta_2)_T\left(\frac{U_T}{U_R}\right)^3 + \left(\frac{C_d}{H_{32}}\right)_m\left(1+\frac{U_T}{U_R}\right)\left[1+\left(\frac{U_T}{U_R}\right)^2\right]\frac{l_2}{4} \tag{17}$$

Horton[3] recommended a value of 0.0182 for $(C_d)_m$, which corresponded to an asymptotic mixing layer. Vincent de Paul[9] computed the dissipation coefficient using a polynomial representation for the separated-flow velocity profiles and an eddy viscosity μ_t equal to $0.06(\rho U \delta_2)$. The resulting value for C_d was 0.0187, which was very close to the value selected by Horton. Roberts,[13] however, argued that this value was not appropriate for reattaching turbulent flows, since it was associated with a flow in which the streamwise pressure gradient was zero. Using separation bubble measurements, he found that $(C_d)_m$ was equal to 0.035, nearly twice Horton's value.

The hot-wire measurements described in Ref. 4 provided an opportunity to test the applicability of Eq. (17) at low Reynolds numbers and to determine appropriate values for $(C_d)_m$. In Fig. 10, the measured growth in δ_2 is compared with that predicted by Eq. (17) using Horton's values for $(C_d)_m$ and $(H_{32})_m$ (i.e., 0.0182 and 1.5). In all of the cases, the momentum thickness growth is underpredicted, often to a significant degree. However, when Roberts' value for $(C_d)_m$ is used instead, the growth in δ_2 is predicted with much greater accuracy (see Fig. 11).

Conditions at Turbulent Reattachment

In order to use Eq. (17), l_2, and thus the location of turbulent reattachment, must be determined. Horton attacked this problem by devising a simple reattachment criterion. By combining the momentum and the mechanical energy integral

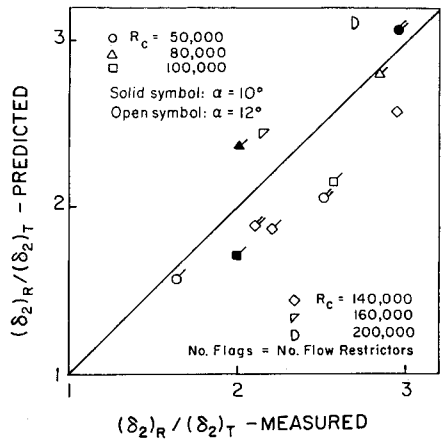

Fig. 11 Measured growth in momentum thickness over bubble's turbulent portion compared with predicted growth using Roberts' recommended value for the dissipation coefficient, $(C_d/H_{32})_m = 0.0233$.

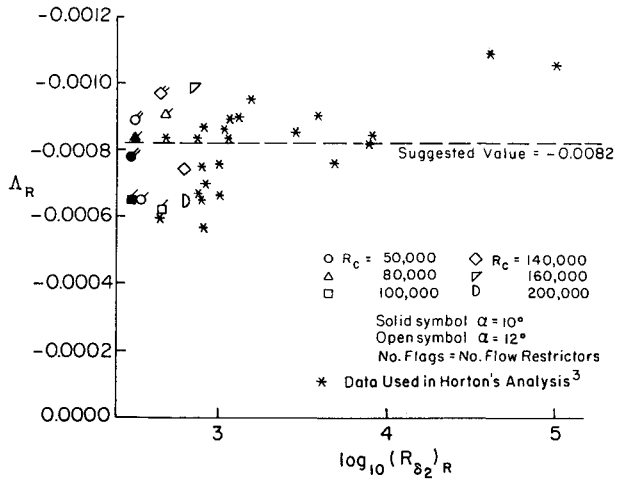

Fig. 12 Horton's reattachment criterion vs momentum thickness Reynolds number at reattachment.

equations and using the characteristics of a velocity profile at reattachment ($C_f = 0$, $dH_{32}/dH_{12} \approx 0$), he derived the following equation:

$$\left(\frac{\delta_2}{U}\right)_R \left(\frac{dU}{dx}\right)_R = -\left(\frac{(C_d)_R}{[H_{32}(H_{12}-1)]_R}\right) \tag{18}$$

Furthermore, he argued that the right-hand side of this expression depends only on the shape of the velocity profile. Finally, he examined several reattachment profiles and found that they were nearly identical. On the basis of these data, Horton suggested that the velocity profile at reattachment is universal. Thus, the right-hand side of Eq. (18) was shown to be constant. Horton calculated the value of this constant by taking $(H_{12})_R$ and $(H_{32})_R$ to be 3.5 and 1.5, respectively. The dissipation coefficient at reattachment was calculated by neglecting viscous contributions to τ and by assuming that the eddy viscosity is equal to $0.02(\rho U \delta_1)$. The resulting value of $\Lambda_R = (\delta_2/U)_R\,(dU/dx)_R$ was -0.00592. However, values of Λ_R obtained from 22 experiments involving separation bubbles as well as flow reattaching downstream of backward-facing steps and roughness elements indicated that -0.00592 was not representative of most of the data. Instead, Horton found that Λ_R ranged from -0.0057 to -0.0109. After examining the frequency distribution of the data, he concluded that the variation was due to random error in the experiments and selected the mean value (-0.0082) as his reattachment criterion. Additional measurements were added to this data base

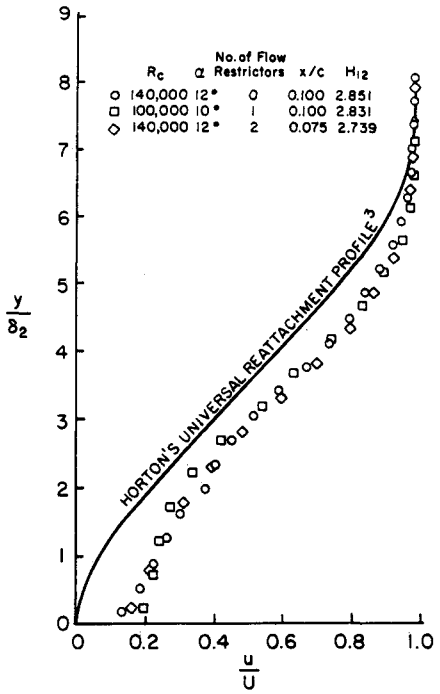

Fig. 13 Examples of velocity profiles at reattachment compared with Horton's universal reattachment profile.

by Roberts,[13] which resulted in a new mean of -0.0075. However, Roberts found that Horton's semiempirical method was more successful in predicting the bursting of separation bubbles if the derived value for Λ_R (-0.00592) was used instead.

In Fig. 12, Horton's original data base is shown, with Λ_R plotted $(R_{\delta_2})_R$. In addition to these data, values of Λ_R obtained from O'Meara's measurements[4] are shown. The range of values associated with these data, $-0.0099 \le \Lambda_R \le -0.0060$, is nearly the same as that of Horton's. Furthermore, the mean based on O'Meara's data is -0.0078, which compares favorably with those obtained by Horton and Roberts. Note that O'Meara's data correspond to $303.83 \le (R_{\delta_2})_R \le 732.62$, whereas Horton's are associated with Reynolds numbers of 510–108,000. Thus, the validity of Horton's reattachment criterion has been demonstrated at somewhat lower Reynolds numbers. Of course, this is not very surprising, since Horton's original data base does not reveal a noticeable variation of Λ_R with $(R_{\delta_2})_R$.

Reattachment criteria also have been developed by van Ingen and Boermans[10] and Vincent de Paul.[9] Van Ingen has established that, at reattachment, the external velocity must satisfy the relationship prescribed by Stratford[28] for a turbulent boundary layer with continuously zero skin friction. Vincent de Paul associated reattachment with H_∞ attaining a value of 4.1. Neither criterion has been examined at this time using O'Meara's data.

Once the reattachment point has been determined, conventional integral methods can be used to evaluate the downstream turbulent boundary-layer growth. In order to initiate the calculations, starting values for various boundary-layer parameters such as H_{12}, H_{32}, and C_d are needed. Horton's concept of a universal reattachment velocity profile is certainly appealing since it simplifies the problem of determining the values of these parameters. In Fig. 13, Horton's universal reattachment profile is plotted. This curve was based on nine velocity profiles, which were the result of the following types of reattaching flows[3]: flow behind an aft-facing step (one case), flow downstream of a two-dimensional roughness element (one case), and swept separation bubbles (seven cases). Also shown in the figure are three of O'Meara's hot-wire profiles. These were selected because they were obtained at

locations very close to the estimated reattachment points. Although the three tend to collapse into a single curve, the resulting curve differs appreciably from Horton's universal profile. O'Meara's profiles are fuller in shape than Horton's mean curve, with higher velocities near the wall. This results in lower values of H_{12} (about 2.8, compared with 3.5 for Horton's profile). Of particular significance is that Horton's universal profile clearly exhibits a zero slope at the wall, a necessary condition for flow reattachment. On the other hand, O'Meara's profiles seem more representative of flow downstream of reattachment. This suggests that the reattachment locations were not correctly determined. If true, it may be the result of not having enough points to accurately define the dividing streamline geometry near reattachment. It also may indicate that the method of determining the height of the dividing streamline is not sufficiently accurate. On the other hand, O'Meara's profiles may actually correspond to reattachment. In this case, the profiles may have been distorted near the wall due to the type of measuring technique used. Because of the single hot-wire's inability to sense flow direction, errors in the magnitude of both the mean and fluctuating parts of the local flow velocity can occur. This will happen whenever the absolute value of the fluctuating component is larger than that of the mean. Thus, a measurement error of this type is likely to be confined near a solid boundary where the mean component is small. If the profiles shown in Fig. 13 are modified near $y = 0$ so that they look more like reattachment profiles, the resulting values of $(H_{12})_R$ and $(H_{32})_R$ are about 3.4 and 1.5, respectively. Therefore, assuming that measurement errors did occur near the airfoil's surface at reattachment, it appears that Horton's recommended values for $(H_{12})_R$ and $(H_{32})_R$ are consistent with the three reattachment profiles shown in Fig. 13.

For test conditions other than those represented in Fig. 13, values of $(H_{12})_R$ and $(H_{32})_R$ were interpolated from O'Meara's measurements. Although $(H_{32})_R$ was approximately equal to 1.5, as suggested by Horton, $(H_{12})_R$ ranged 2.162–3.4976. Despite the fact that the wide range in $(H_{12})_R$ may be due to the measurement uncertainties described above, there is additional evidence that $(H_{12})_R$ may indeed take on a broad range of values. References 24, 25, and 29 provide eight cases of separation bubble measurements for which the local flow direction was determined. These measurements indicate that $(H_{12})_R$ can range from 1.54–4.37, with an average value of 3.03. At present, it is not clear how significant this finding is in terms of boundary-layer calculations downstream of a separation bubble. It may be sufficient to use a typical value for H_{12} at reattachment such as 3.0 or 3.5.

Conclusions

Integral boundary-layer-type methods have, in the past, been found useful for predicting some of the characteristics of separation bubbles. Their major deficiency lies in their reliance on experimental data. Hence, the methods need to be tested carefully whenever they are applied to new situations. The purpose of this article was to examine the applicability of these methods to the problem of separation bubbles formed on airfoils at low Reynolds numbers. Available measurements of the flow in the vicinity of separation bubbles had the disadvantage of being obtained with a single hot-wire anemometer. As a result, regions of reversed flow could not be accurately determined, thus introducing the possibility of errors in the derived boundary-layer parameters. In order to correct this problem, a method was devised that could locate the height of the dividing streamline within a velocity profile without the knowledge of the local flow direction. This technique was used to correct the boundary-layer parameters obtained in the low Reynolds number experiments and to estimate the locations of laminar separation and turbulent reattachment on the airfoil.

From the low Reynolds number data, it was discovered that a significant (over sixfold) increase in the momentum thickness can occur in a separation bubble between the positions of laminar separation and transition. The initial stages of the growth were found to be similar to theoretical results for a laminar half-jet and appear to be governed by the momentum thickness Reynolds number at separation. This parameter also was found to have a noticeable effect on the Reynolds number based on the length of a bubble's laminar portion. Data from several sources indicate that this transition Reynolds number ranges from 10,000–69,000 for momentum thickness Reynolds numbers between 28 and 750. It is acknowledged, however, that factors such as the turbulence level in the freestream, the boundary-layer shape factor at separation, and the separation angle also can have a significant effect on the transition Reynolds number. In order to confidently isolate the effect of these parameters on the phenomenon of transition, experiments must be devised in which the freestream disturbance environment, Reynolds number, and pressure distribution upstream of separation can be carefully controlled. This is a very difficult task in the case of low Reynolds number airfoil flows since the pressure distribution is affected by conditions at the airfoil's trailing edge, which are in turn affected by the extent of the separation bubble.

Although Reynolds number effects were found to be significant in the laminar portion of separation bubbles, this was not found to be the case in regions of turbulent flow. The momentum thickness growth was predicted reasonably well using a simple formula based on the energy equation and Robert's recommended value for the dissipation coefficient. Also, the turbulent reattachment criterion devised by Horton was verified at somewhat lower Reynolds numbers. However, Horton's conclusion that the velocity profile at reattachment is universal has not been verified. Values of the boundary-layer shape factor at reattachment ranged from 2.162–3.4976. Although it is possible that measurement uncertainties were responsible for the wide range in H_{12}, the results are consistent with separation bubble measurements obtained by other investigators. It is recommended that a value of 3.0 or 3.5 be used for $(H_{12})_R$ as a starting value for boundary-layer calculations downstream of reattachment.

Acknowledgments

This research was supported under Grant NSG-1419 by the NASA Langley Research Center, where D. M. Somers served as the technical monitor, and the Department of Aerospace and Mechanical Engineering, University of Notre Dame.

References

[1]Schmidt, G. S., "The Prediction of Transitional Separation Bubbles at Low Reynolds Numbers," Ph.D. Dissertation, University of Notre Dame, Notre Dame, IN, Dec. 1986.

[2]Clayton B. R. and Massey, B. S., "Flow Separation in an Aerofoil Cascade," *Journal of the Royal Aeronautical Society,* Vol. 71, Aug. 1967, pp. 559–565.

[3]Horton, H. P., "Laminar Separation Bubbles in Two and Three Dimensional Incompressible Flow," Ph.D. Thesis, University of London, London, 1968.

[4]O'Meara, M. M., "An Experimental Investigation of the Separation Bubble Flow Field Over an Airfoil at Low Reynolds Numbers," M.S. Thesis, University of Notre Dame, Notre Dame, IN, 1985.

[5]Stewartson, K., "Further Solutions of the Falkner-Skan Equation," *Proceedings of the Cambridge Philosophical Society,* Vol. 50, 1954, pp. 454–465.

[6]Schlicting, H., *Boundary Layer Theory,* McGraw-Hill, New York, 1979.

[7]Green, J. E., "Two-Dimensional Turbulent Reattachment as a Boundary-Layer Problem," AGARD CP 4, Pt. I, 1966, pp. 393–428.

[8]Gault, D. E., "An Experimental Investigation of Regions of Separated Laminar Flow," NACA TN 3505, Sept. 1955.

[9]Vincent de Paul, M., "Prevision du Decrochage d'un Profil d'Aile en Ecoulement Incompressible," AGARD CP 102, 1972, pp. 5-1 to 5-15.

[10]van Ingen, J. L. and Boermans, L. M. M., "Research on Laminar Separation Bubbles at Delft University of Technology in Relation to Low Reynolds Number Airfoil Aerodynamics," *Proceedings of Con-*

ference on Low Reynolds Number Airfoil Aerodynamics, University of Notre Dame, Notre Dame, IN, UNDAS-CP-77B123, 1985, pp. 89–124.

[11]Russell, J. M., "Length and Bursting of Separation Bubbles: A Physical Interpretation," NASA CP 2085, Pt. I, 1979, pp. 177–201.

[12]Christian, W. J., "Improved Numerical Solution of the Blasius Problem With Three-Point Boundary Conditions," *Journal of the Aerospace Sciences,* Vol. 28, Nov. 1961, pp. 911–912.

[13]Roberts, W. B., "A Study of the Effect of Reynolds Number and Laminar Separation Bubbles on the Flow through Axial Compressor Blades," DSc Thesis, Université Libre de Bruxelles, Institut d'Aeronautique, and von Kármán Institute for Fluid Dynamics, Brussels, May 1973.

[14]Davis, R. L., Carter, J. E., and Reshotko, E., "Analysis of Transitional Separation Bubbles on Infinite Swept Wings," AIAA Paper 85-1685, July 1985.

[15]Tani, I., "Boundary Layer Transition," *Annual Review of Fluid Mechanics,* Vol. 1, 1969, pp. 169–196.

[16]Crimi, P. and Reeves, B. L., "Analysis of Leading-Edge Separation Bubbles on Airfoils," *AIAA Journal,* Vol. 14, Nov. 1976, pp. 1548–1555.

[17]Carmichael, B. H., "Low Reynolds Numbers Airfoil Survey," Volume 1, NASA CR-165803, Nov. 1981.

[18]Sandborn, V. A., "Characteristics of Boundary Layers at Separation and Reattachment," College of Engineering, Colorado State University, Fort Collins, Res. Memo. 14, Feb. 1969.

[19]Dobbinga, E., van Ingen, J. L., and Kooi, J. W., "Some Research on Two Dimensional Laminar Separation Bubbles," AGARD CP 102, 1972, pp. 2-1 to 2-9.

[20]Dryden, H. L., "Transition from Laminar to Turbulent Flow," *Turbulent Flows and Heat Transfer,* Princeton University Press, Princeton, NJ, 1959.

[21]Woodward, D. S., "An Investigation of the Parameters Controlling the Behaviour of Laminar Separation Bubbles," Royal Aircraft Establishment, Farnborough, Hampshire, England, Tech. Memo. Aero 1003, Aug. 1967.

[22]Schubauer, G. B., "Air Flow in the Boundary Layer of an Elliptic Cylinder," NACA Rept. 652, Aug. 1938.

[23]Brendel, M., "Experimental Study of the Boundary Layer on a Low Reynolds Numbers Airfoil in Steady and Unsteady Flow," Ph.D. Dissertation, University of Notre Dame, Notre Dame, IN, 1986.

[24]Crouch, J. D. and Saric, W. S., "Oscillating Hot-Wire Measurements above an FX63-137 Airfoil," AIAA Paper 86-0012, Jan. 1986.

[25]Mangalam, S. M., Meyers, J. F., Dagenhart, J. R., and Harvey, W. D., "A Study of Laminar Separation Bubble in the Concave Region of an Airfoil Using Laser Velocimetry," American Society of Mechanical Engineers, New York, FED-Vol. 33, Nov. 1985, pp. 265–272.

[26]Gaster, M., "The Structure and Behaviour of Laminar Separation Bubbles," AGARD CP 4, 1966, pp. 813–854.

[27]Crabtree, L. F., "The Formation of Regions of Separated Flow on Wing Surfaces," British Aeronautical Research Council, London, R&M 3122, July 1957.

[28]Stratford, B. S., "The Prediction of Separation of the Turbulent Boundary Layer," *Journal of Fluid Mechanics,* Vol. 5, Jan. 1959, pp. 1–16.

[29]Bell, W. A. and Cornelius, K. C., "An Experimental Investigation of a Laminar Separation Bubble on a Natural Laminar Flow Airfoil," AIAA Paper 87-0458, Jan. 1987.